IPY Developments to Measure Arctic Sea Ice

Cathleen A. Geiger[1], Bruce C. Elder[3], Christian Haas[7], Stefan Hendricks[5], Jenny Hutchings[4], Chandra Kambhamettu[2], Torge Martin[6], Jackie Richter-Menge[3], Joao Rodrigues[8], Nicholas Toberg[8], Mani Thomas[2], Peter Wadhams[8], John Weatherly[3]

[1]Geography and [2]Computer and Information Science, University of Delaware, DE, USA; [3]Cold Regions Research and Engineering Laboratory, Hanover, NH, USA; [4]University of Alaska, Fairbanks, USA;[5]Alfred Wegener Institute, Bremerhaven, Germany; [6]IFM-GEOMAR, Leibniz Institute of Marine Sciences, Kiel , Germany; [7]University of Alberta, Edmonton, CA; [8]Department of Applied Mathematics and Theoretical Physics, University of Cambridge, UK

ABSTRACT

This poster demonstrates a range of tools, techniques, and capabilities that have been developed over the course of three Arctic projects supported through NSF and NASA during the IPY years. The main point of this poster is to convey the sense of complexity involved in direct measurements of sea ice. In particular, we focus on efforts to resolve a number of important differences between instruments and/or techniques; differences which have a profound impact on the long-term monitoring and quantification of sea ice mass balance. Several publications are complete, under review, or accepted manuscripts with highlights from five example publications shown here.

P1. Telemetry Techniques

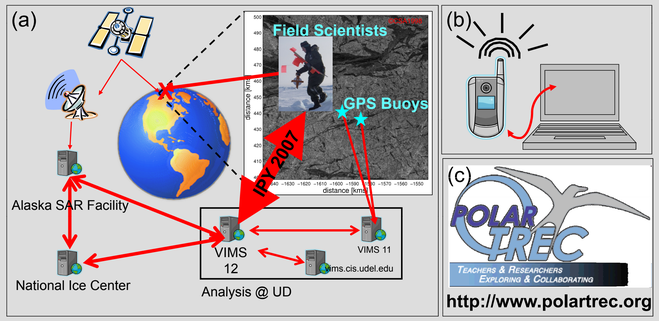

Figure 1: The combination of (a) large land-based infrastructure plus (b) light-weight, high powered portable equipment makes today's field work more time and cost effective than ever before. These capabilities allowed for huge advancements not only in science but also in (c) outreach and education with high school teachers joining us in the field while both scientists and their field events participate live in the classroom. One of the landmark advancements of IPY has clearly been an increase in near-real time polar science and communication.

P2. Motion Tracking Products

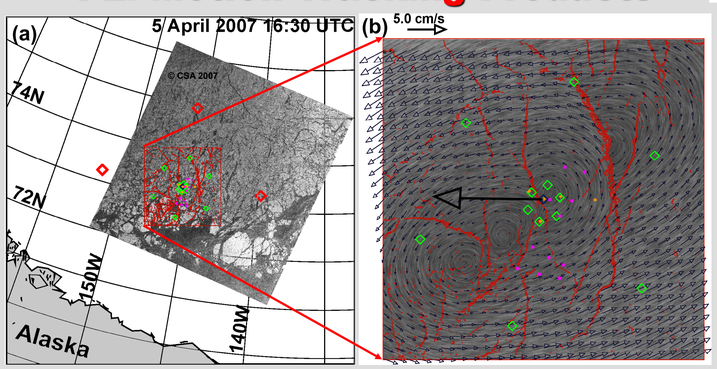

Figure 2: We are exploring new ways to effectively combine high spatial (50m), low temporal (1-3 day) resolution active microwave imagery and low spatial (point), high temporal (<1 hr) resolution telemetry GPS buoys. These efforts are aimed at refining satellite motion products down to the scale of field observations to support both scientific research and logistics as demonstrated in panel (a). As summer sea ice decreases, ship traffic in the Arctic will naturally increase. It is our hope that these developments may some day serve as operational navigation aids throughout the Arctic as well as integrative diagnostic tools for understanding changes in the dynamic component of sea ice mass balance as demonstrated in panel (b). For more information on this and other computer visions advancements see http://www.eecis.udel.edu/wiki/vims/.

P3. Thickness Analysis

Thickness Measurements & Resolution Error

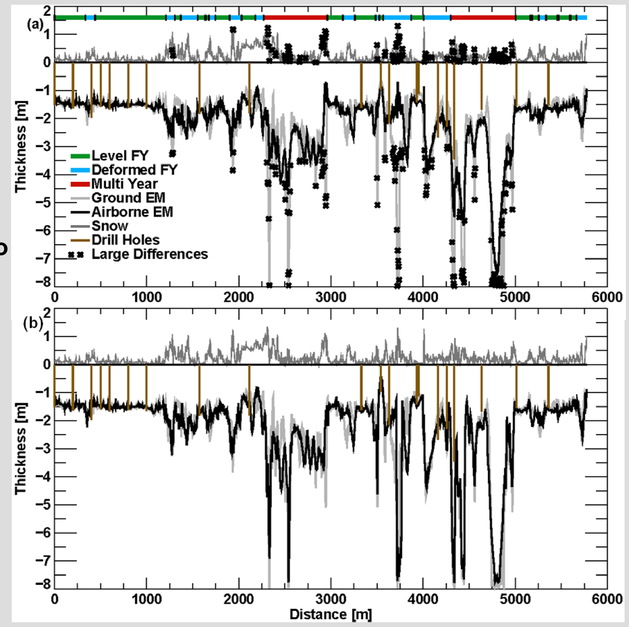

Figure 3.1: Impact and correction of features aliased in large footprint instruments. Panel (a) shows two coincident Electromagnetic Induction (EMI) thickness retrievals during SEDNA. The black profile is Airborne EMI with 40m footprint while the grey profile is Ground EMI with 4m footprint. Each instrument is corrected for bias error relative to level ice as per standard procedure. Panel (b) shows results after applying additional correction due to resolution error. See heuristic model for explanation.

Heuristic Explanation: Spatial Aliasing

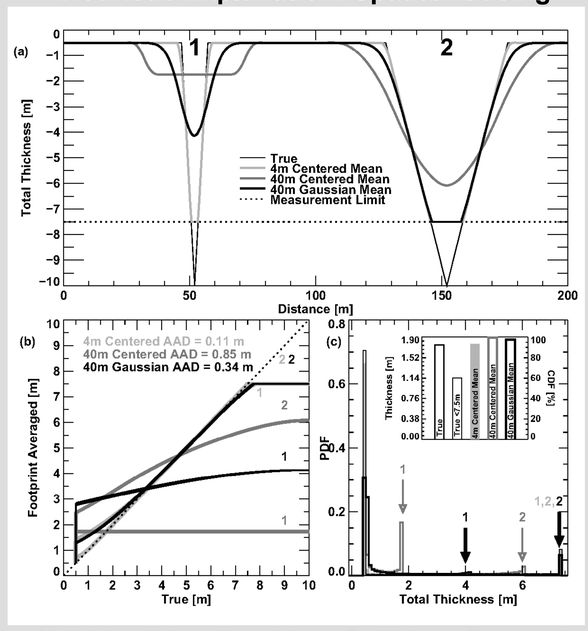

Figure 3.2: Heuristic model characterizing resolution error. Panel (a) shows profiles constructed at 10 cm resolution for level ice and two simple triangular ridges. Ridge 1 represents narrow First Year Deformed (FYD) ice while Ridge 2 represents a MultiYear (MY) floe wider than an Airborne EMI footprint. The dashed horizontal line lets us consider the impact of instrument depth limits. Panels (b) and (c) show scatter plot and thickness distributions, respectively. Aliasing of thick ice manifests as a skewing in scatter plots and artificial peaks in thickness distributions with little impact to integrated thickness as a volume proxy. Surface topography responds similarly.

P4. Comparison of Observations and Models

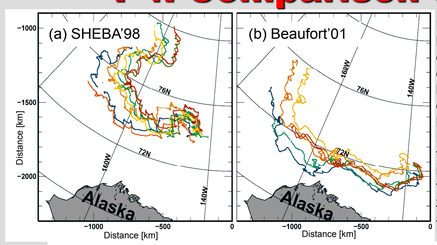

Figure 4.1: Drift trajectories of stress buoy arrays for (a) 1998 and (b) 2001 deployment campaigns. Both arrays were deployed near 140W in Autumn and lasted until Spring breakup. The relevant difference is the deployment of SHEBA buoys deep into the gyre while the Beaufort'01 experiment deployed closer to the coast. Both circulation patterns reflect typical gyre circulation patterns for this region with a strong coastal shear zone stretching the Beaufort'01 array along the coast.

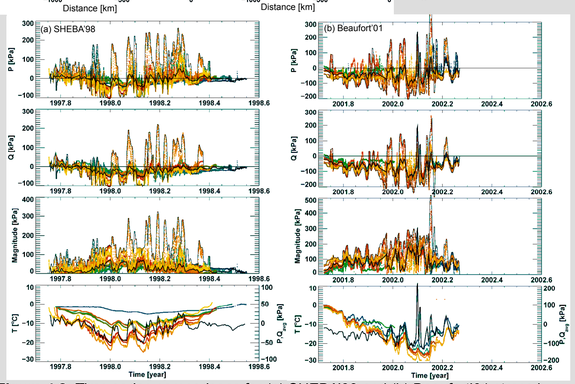

Figure 4.2: Time series comparisons for (a) SHEBA'98 and (b) Beaufort'01 stress buoy arrays. The *P* and *Q* major and minor stresses undergo similar annual cycle changes including reduced average stress (thick black line of sliding daily averages) into the winter months as the temperature drops and ice compresses thereby reducing the overall stress state. The thick black line in the temperature time series is the sum of the absolute value of P and Q which strongly correlate with ice temperature indicating a strong thermal stress contribution. At the same time, variability grows through the winter as seen by the increased maxima and minima (thin black line tracked as a daily sliding maximum magnitude). These oscillations contribute to the annealing of the ice as it is broken and reworked again and again on synoptic time scales. This annealing process is important because it changes the composition of the ice and mechanically redistributes the ice thickness. Hence, these annealing events are useful processes to compare with model outputs including fundamental insight between sea ice material behavior and ice volume changes.

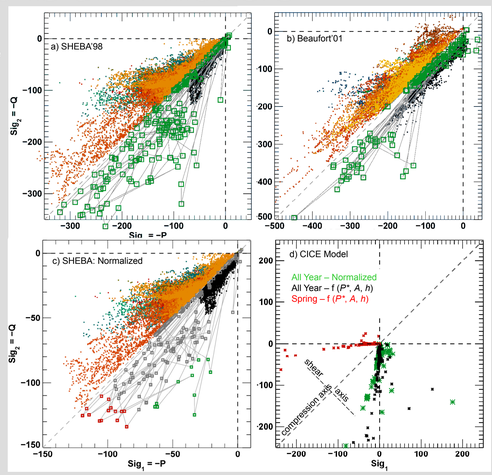

Figure 4.3: Principal stress states. Panels (a) and (b) show annual cycle observed stresses. Colored points match buoys of earlier figures while black points show spatial averages from all stress buoys at each time. Grey lines track daily maximum magnitudes with end points marked by green boxes. These maximum excursions demonstrate the path of stress states during the annealing process. Two dominant patterns are present: (1) smaller stress maxima along the compression axis similar to the Cavitating Fluid Rheology, and (2) Mohr Coulomb paths or paths within a confined ellipse. Occasionally there are paths perpendicular to the compression axis along the shear axis. Differences in envelope shape may be caused by interannual variability or proximity to the nearby coastline (e.g., narrower envelope with large triangular excursions resembling the cap of a Mohr Coulomb envelope). Normalizing the SHEBA results in panel (c) using thickness, we identify stress states close to the annual maximum (red boxes). It is difficult to measure stress states close to yielding and hence we suspect that much more data is needed to develop the full envelope. To be successful, such efforts must include coincident thickness and ice concentration observations to compared with models as seen in Panel (d) where the envelope of the CICE model is much wider than all observed stresses whether normalized or separated by season.

P5. Scale Analysis

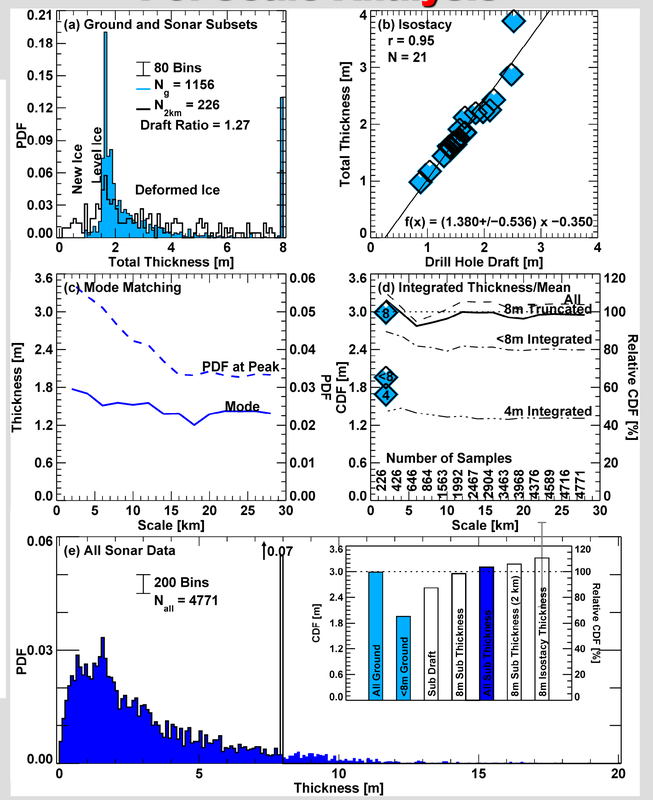

Figure 5. Scale analysis. Panel (a) shows total thickness probability distribution (PDF) from the ground survey. We use these measurements to calibrate submarine draft to total thickness using a mode-matching algorithm. This method has much less uncertainty than the typical isostacy approach as seen in the inset of panel (e). Uncertainty denoted by the vertical uncertainty bar of computed white noise as a function of bin number. Panel (b) shows isostacy relations between draft and total thickness at drill-hole sites with a higher uncertainty using this method versus mode matching. Panel (c) summarizes analysis as a function of scale. Panel (d) compares integrated thickness (mean) of ground survey (diamonds) and subsamples from submarine sonar at scales relative to the camp. Panel (e) shows total thickness for all sonar data using the draft factor in panel (a) with the bold-line distribution showing the 8m truncated version for direct compatibility with the ground survey. Panel (e) insert shows example integrated thickness to illustrate differences in methodology and uncertainty. The grey uncertainty bar on the 8m isostacy case is the range of integrated thickness when propagating the uncertainties in the slope shown in panel (b).

6. Products & Publications

Archive: J. Hutchings, C. Geiger, J. Richter-Menge, A. Roberts, P. Clemente-Colon, M. Doble, B. Elder, R. Forsberg, R. Gens, K. Giles, C. Haas, S. Hendriks, B. Holt, N. Hughes, C. Khambhamettu, R. Kwok, T. Martin, A. Orlich, D. Perovich, M. Pruis, I. Rigor, H. Skourup, H. Simmons, P. Wadhams, J. Wilkinson, H. J. Zwally. 2011. Data archive from International Polar Year Project - SEDNA: Sea ice Experiment - Dynamic Nature of the Arctic. http://dw.sfos.uaf.edu/sedna. IPY Archive Number: XXXX.

P1: Huffman, L., J. Baeseman, K. Timm, J. Warburton, with contributions from M. Albert, M. H. Almeida, P. Azinhaga, R. Bindschadler, P. Dionísio, R. Frisch-Gleason, C. Geiger, C. Hamilton, T. Haste, J. Hubbard, M. Jeffries, L. Murphy, M. M. Passas , M. Prevenas, M. Raymond, R. Salmon, F. Silva, C. Teixeira, K. Tolstein, B. Trummel, J. Xavier, S. Zicus (2010), Chapter 2: Tips and Tricks in the Classroom, in: Polar Science and Global Climate - An International Resource for Education and Outreach. B. Kaiser (ed), Pearson, London, 129-141. (Publication release date May 2010 – Oslo IPY Conference).

P2: Thomas, M. V., C. Kambhamettu, C. Geiger (2011), Motion tracking of discontinuous sea ice, Transactions on Geoscience and Remote Sensing, Accepted Manuscript: TGRS-2010-00277.R2.

P3: Geiger, C. A., J. Richter-Menge, S. Hendricks, C. Haas, H.-R. Mueller, T. Martin, and B. Elder (*2012*), Impact of instrument footprints from electromagnetic induction sea ice thickness retrievals, under review *to Journal of Geophysical Research – SEDNA special issue,* Paper No. 2011JC007149..

P4: Geiger, C. A., J. W. Weatherly, J. Richter-Menge, and B. Elder (in preparation), Stress comparison between year-long buoy arrays and the CICE model, *for J. Geophys. Res.*

P5: Geiger, C. A., J. Richter-Menge, T. Deliberty, B. Elder, J. Hutchings, A. Lawson, J. Rodrigues, N. Toberg, and P. Wadhams (2010), A Case Study Testing the Impact of Scale on Arctic Sea Ice Thickness Distribution, Proceedings of 20th IAHR International Symposium on Ice held in Lahti, Finland, June 14 to 18, 2010, 15 pages.

Funding provided through NSF ARC-0612527, 0611991, 0612105; OPP-0703682, 0736030, 0636726; EU Damocles, and NASA NNX07AL77G. Many thanks to the ARCUS program PolarTREC and NSF for their support of Vermont high school teacher Robert Harris who participated under the SEDNA project.